

Analysis of PV Arrays for Residential Applications Using a Three-Phase Step-Up Isolated DC-DC Converter with High-Frequency Transformer

Renan Diego de Oliveira Reiter¹, Leandro Michels², Adriano Pères¹, Sérgio Vidal Garcia Oliveira¹
¹ Universidade Regional de Blumenau (FURB), ² Universidade Federal de Santa Maria (UFSM)
E-mail: renandiego@gmail.com, leandromichels@gmail.com, aperes@furb.br, svgo@furb.br

Abstract- This paper has the objective of performing analyses with the series, parallel, and multi-string array with a few photovoltaic (PV) modules under partial shading conditions, with these analysis it is chosen an array of PV modules with total power installed of 6kW for powering a residence using a single DC-DC converter. With the chosen array configuration, it is performed the design of the three phase step-up isolated DC-DC converter with high frequency transformer, in charge of tracking the maximum power point and to provide energy to a grid-connected inverter. Simulation results are presented to demonstrate the advantages of the parallel array using the DC-DC converter.

I. INTRODUCTION

The growing global climate changes have drawn much attention to the replacement of energy from fossil fuels by solutions with renewable energy sources. One of the most promising is the use of photovoltaic (PV) energy because does not emit CO₂ during its operation, requires little maintenance, has simple installation, among other advantages [1], [2].

Photovoltaic systems can be classified taking into consideration different aspects such as the application, structure and topology [3]. Grid-connected photovoltaic systems (GCPS) have been received most interest due attractiveness for distributed generation (DG) in residences that intent to be environmentally friendly with zero carbon emission [4]. In this direction, several government incentive programs were created in the U.S., Spain, Japan, and Germany, such as the 100,000 Roof Solar Electricity Programme [5], [6]. These systems are designed to supply energy directly to end users in low voltage (LV). Moreover, if the PV system generates more energy than consumer demands, the GCPS inject the exceeded energy into the grid.

Several concepts of GCPS have been proposed in the literature: central inverters, string inverters, multi-string inverters, team concept, AC module, among others [7], [8]. These schemes show different characteristics in relationship to the Fill Factor (FF) [9], energy efficiency conversion, security, hardware complexity, modularity, scalability, reliability, simplicity of installation and maintenance, cost, and so on. As a result, the choice of the most advantageous scheme is a decision case-by-case.

Central inverter (CI) schemes have some advantageous characteristics such as: low cost of the converter, reduced system complexity, reliability, easy installation and

maintenance. This scheme had been used in most commercial systems.

Central inverters can be classified by the number of power processing stages: i) single-stage, where a single DC-AC inverter handles the MPTT and grid current control; ii) dual-stage single-string, where a DC-DC converter is responsible for the MPPT and a DC-AC inverter controls the grid current, and iii) dual-stage multi-string, where each PV module or string are connected to a dedicated DC-DC converter that is connected to a DC-AC inverter [10].

Single-stage CI topologies uses larger number of PV modules in series for direct connection of PV to inverter. This arrangement increases the conversion efficiency but reduces the FF of available solar energy when some modules are partially shaded [11]. Some dual-stage CI topologies are more advantageous for PV applications under partial shading: i) single-string topologies with parallel arrangement of PVs, and ii) multi-string topologies. These topologies are suitable for residential applications because increase significantly the FF under partial shading.

Parallel arrangements have some advantages in relation to series ones: i) improvement of the maximum power point tracking of PVs under partial shading; ii) reduction of PVs losses due to power ripple; iii) greater safety due to smaller voltage on PVs terminals [12], [16]. However, the main drawback of parallel arrangements is the necessity of a conversion stage with high voltage gain, which reduces the system efficiency [9].

Centralized GCPS can be also classified in relation to galvanic isolation: isolated and non-isolated. The advantage of non-isolated GCPS is the high energy conversion efficiency. Nevertheless, non-isolated schemes present difficult to meet some standards such as IEEE 1374/1998 [16] associated to leakage current, grounding of PVs, and risk of electric shock [13].

This manuscript proposes a GCPS based on central inverter with dual-stage single-string power processing stages with galvanic isolation based on parallel PVs arrangements. This topology uses a Step-Up DC-DC Converter with a Three-Phase High-Frequency Transformer (SDCTHT) in the input stage [15]. This topology has the following advantageous characteristics: i) galvanic isolation; ii) high-voltage gain (up to 10x) in a single stage, which is suitable for parallel or series/parallel PV arrays with few PVs in series; and iii) reduced input current ripple which allows the

reduction of input capacitors. It is used a buck converter as a snubber to minimize the peak voltage across the switches.

The paper is organized as follows. First is analyzed de FF for 6 PVs modules employing series, parallel and multi-string arrangements, where is demonstrated the advantages of using parallel array in partial shading conditions. From this analysis is determined the better array for a set of 45 PV modules to minimize the effects of partial shading. So the SDCTHT converter is designed to operate under a wide range of ambient temperatures and solar irradiation. Simulation results are presented to demonstrate the design procedure, and finally, experimental results are presented.

II. COMPARATIVE ANALYSIS OF PV ARRAYS

In this section is presented a comparative analysis of the

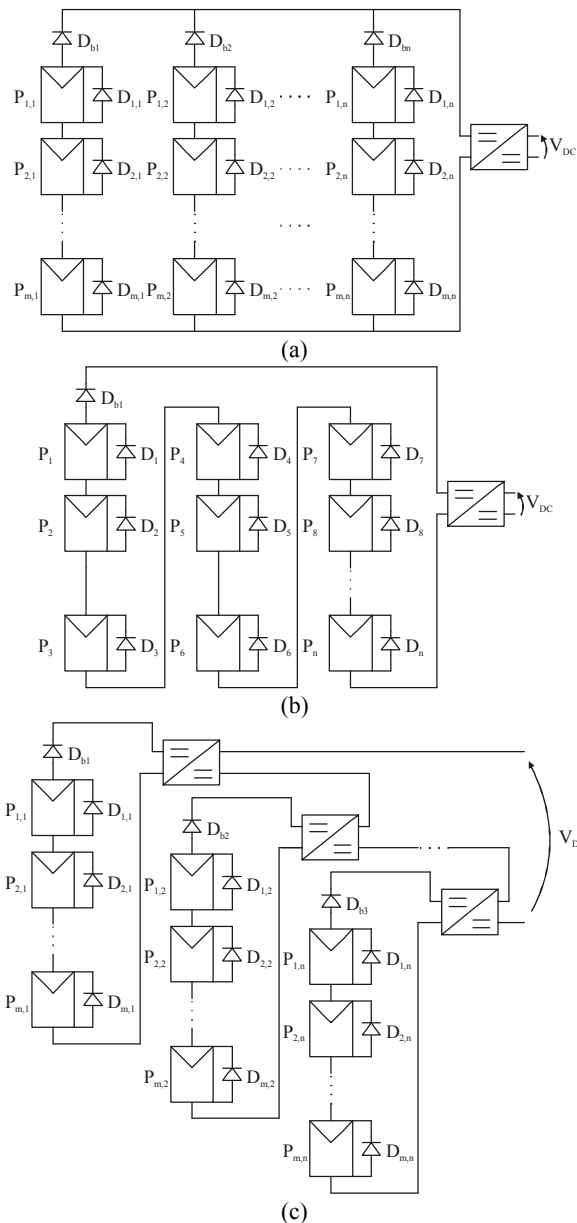


Fig. 1. PV arrangements. (a) Parallel single string. (b) Series single-string. (c) Multi-string.

input converter of dual-stage PV schemes: The following configurations have been considered: parallel single-strings (PSS), series single-string (SSS), and multi-string (MS).

Fig. 1 shows the three proposed arrangements. For comparative analysis it is considered 6 PV modules in each configuration. Fig. 1(a) shows the PSS configuration consisted of two arrays of three modules connected in series (first array: $P_{1,1}, P_{2,1}, P_{3,1}$; second array $P_{1,2}, P_{2,2}, P_{3,2}$). Fig. 1(b) presents the SSS configuration, where the modules are named $P_1 - P_6$. The MS configuration is illustrated in Fig. 1(c). This PV array has similar configuration of parallel one, but now each array is connected to its own DC-DC converter (first converter: $P_{1,1}, P_{2,1}, P_{3,1}$; second converter $P_{1,2}, P_{2,2}, P_{3,2}$).

The analysis is based on simulation results. The PVs considered in this analysis are the Kyocera KC130TM, whose main characteristics for an irradiation of 1000W/m^2 and 25°C are found in [14]. The behavior of blocking diode (D_b) and the bypass diodes is approximated by an ideal diode with a voltage drop of 0.7V . Moreover, it is assumed that all converters have the same efficiency.

Table I presents two different scenarios that had been considered to analyze the effect of partial shading in these PVs configurations. It is assumed that all PVs have 25°C .

Test 1 assumes that all PV modules of one array of PSS and MS are shaded. Fig. 2 shows $P-V$ curves for this test. One can observe that SSS array has multiple peaks of maximum power point (MPP) due to different irradiation in the same array. Table II presents a comparison of FF at maximum power point in these arrangements. As can be seen, both PSS and MS arrays have the same FF, which is almost independent of the shading. On the other hand, SSS array present a lower FF which is highly dependent of the shading.

Test 2 also assumes three PV modules are shaded, but now one array of PSS and MS have two modules shaded while other array have one module shaded. Fig. 3 shows $P-V$ curve for this test. One can observe that PSS, SSS, and MS arrays have multiple peaks of maximum power due to different irradiation in the same array. Table III present a comparison of FF at maximum power point in these arrangements. As can be seen, SSS arrays have a higher FF due to lower losses in the blocking diodes. Moreover, MS array have a FF significantly higher than PSS array.

From this analysis we obtain that: i) SSS and MS arrangements have higher FF then PSS when all arrays have some modules shaded; ii) SSS have a wider input voltage range at MPP; iii) MS and PSS have similar FF when shading

TABLE I
IRRADIATION (W/m^2) OF PVs IN EACH SIMULATION.

Test	$P_{1,1}$	$P_{2,1}$	$P_{3,1}$	$P_{1,2}$	$P_{2,2}$	$P_{3,2}$
1-A	800	800	800	1000	1000	1000
1-B	600	600	600	1000	1000	1000
1-C	200	200	200	1000	1000	1000
2-A	1000	800	800	1000	1000	600
2-B	1000	500	500	1000	1000	200
2-C	1000	300	300	1000	1000	100

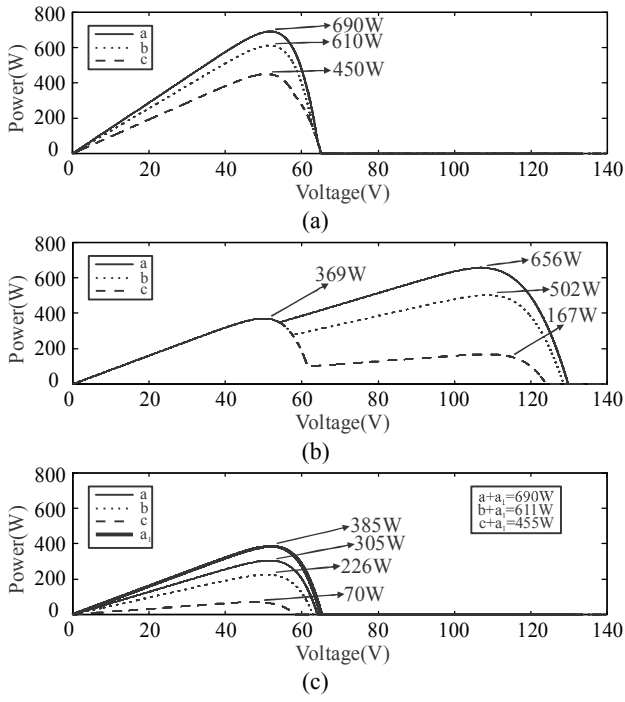


Fig. 2. P-V curves for Test 1: (a) PSS array. (b) SSS array. (c) MS array.

TABLE II
TEST 1.

Shading	PSS		SSS		MS	
	Power	FF	Power	FF	Power	FF
A-800W/m ²	690W	98,7%	656W	93,8%	690W	98,7%
B-600W/m ²	610W	98,5%	502W	81,1%	611W	98,7%
C-200W/m ²	450W	97,6%	369W	80%	455W	98,7%

occurs in all modules of each array; and iv) MS have better FF when several different modules are shaded. Therefore, one can conclude that PSS have a little lower FF than MS when the arrays have few modules in series.

III. CHOICE OF ARRANGEMENT OF PV MODULES

This section investigates the choice of arrangement of modules for PSS PV configuration. The analysis is performed for a PV arrangement for residential applications with approximate power peak of 6kW. Three series/parallel arrangements of PV modules are analyzed: 3x15, 4x11 and 5x9.

Fig. 4 shows the arrangements of PV modules analyzed in this paper, where the modules colored in gray and black are under partial shading. Two different irradiation patterns have been tested, whose irradiation is defined according to the color of modules in Fig. 4:

- Case a: White: 1000 W/m², Gray: 700 W/m², Black: 700 W/m².
- Case b: White: 1000 W/m², Gray: 700 W/m², Black: 400 W/m².

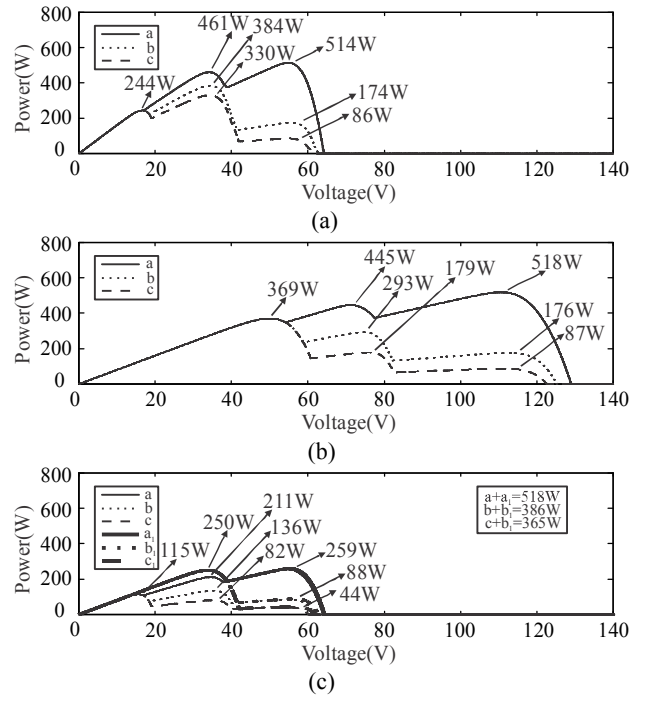


Fig. 3. P-V curves for Test 2: (a) PSS array. (b) SSS array. (c) MS array.

TABLE III
TEST 2.

Shading	PSS		SSS		MS	
	Power	FF	Power	FF	Power	FF
A-800W/m ² and 600W/m ²	514W	79,6%	518W	80,2%	518W	80,2%
B-500W/m ² and 200W/m ²	384W	76,8%	369W	73,8%	386W	77,2%
C-300W/m ² and 100W/m ²	330W	73,5%	369W	82,2%	365W	81,3%

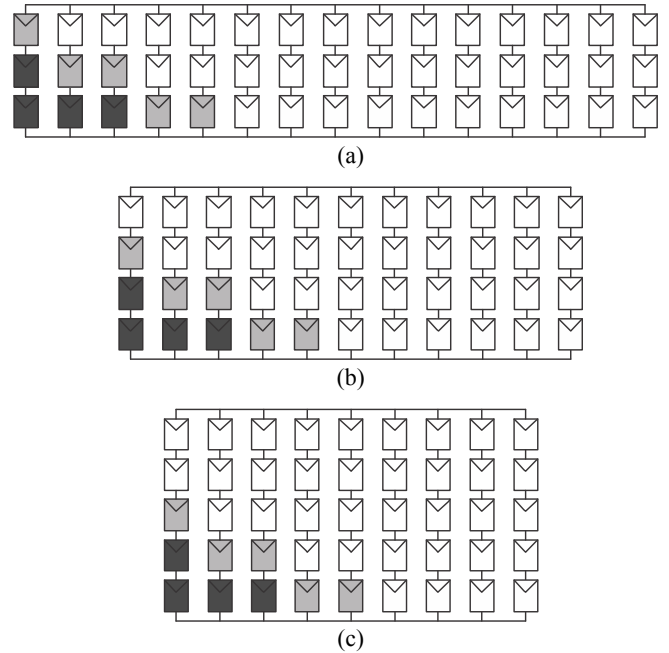


Fig. 4. PV modules arrangements under partial shading. (a) 3x15. (b) 4x11. (c) 5x9.

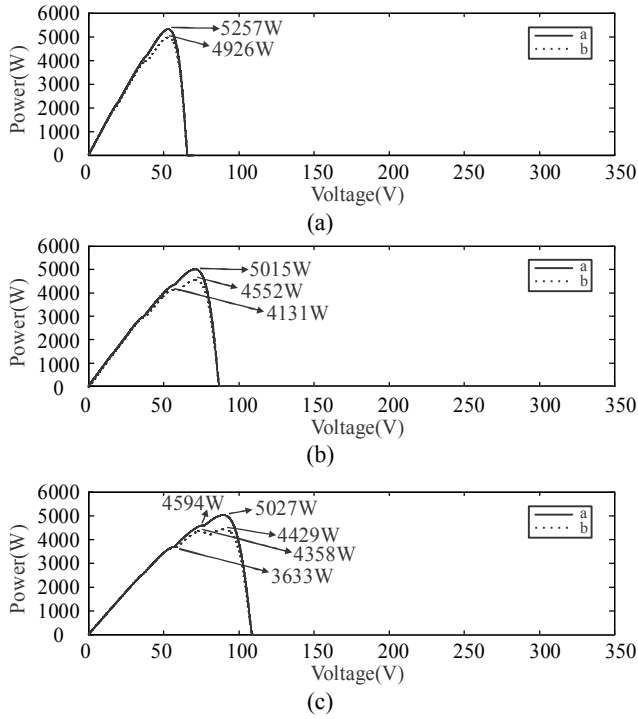


Fig. 5. P-V curves for different arrangements of PV modules. (a) 3x15. (b) 4x11. (c) 5x9.

TABLE IV
COMPARATIVE ANALYSIS OF ARRANGEMENTS 3X15, 4X11 AND 5X9.

Configuration	Power	FF
3x15 – Case a	5257W	95,77%
3x15 – Case b	4926W	92,45%
4x11 – Case a	5015W	93,58%
4x11 – Case b	4552W	87,57%
5x9 – Case a	5027W	90,92%
5x9 – Case b	4429W	82,49%

Fig. 5 shows the P-V curve for the arrangements of PV modules shown in Fig. 4. Table IV present the FF at MPPT for all tests. One can observe that FF is significantly higher for arrangements with fewer modules in series. For instance, from 3x15 to 5x9 one can observe that FF increased more than 5%. Similar results are obtained for other patterns of partial shading.

Moreover, Fig. 5(a) and Fig. 5(c) shows that the input voltage at MPPT condition changes slightly in 3x15

TABLE V
VOLTAGE RANGE OF THE ARRAY 3X15.

Irradiation/Temperature	P_{MPPT}	V_{MPPT}	V_{OC}
1000 W/m ² / 25°C	5852W	52.68V	65.80V
1000 W/m ² / 70°C	4560W	42.38V	55.48V
1000 W/m ² / 0°C	6582W	58.49V	71.07V
100 W/m ² / 25°C	502W	45.57V	53.85V
100 W/m ² / 70°C	365W	34.14V	43.86V
100 W/m ² / 0°C	579W	52.07V	62.35V

TABLE VI
CONVERTER SPECIFICATIONS.

Parameter	Specification
Input power (P)	5852 W
Output voltage (V_o)	360 V
Input voltage (V_{in})	34.14 V ~ 58.49 V
Output voltage variation (ΔV_o)	10 V
Input current variation (ΔI_{in})	2 A
Switching frequency (f_s)	20 kHz
Grid frequency (f_i)	60 Hz

arrangement but significantly in 5x9 arrangement. As a result, the DC-DC converter can be designed for a smaller range of input voltages.

Due these advantages, as well as the advantages related to lower risk of electrical shocks and cost of protection equipment, the arrangement 3x15 have been chosen in this project.

IV. INPUT-STAGE CONVERTER DESIGN

This section present the design of input stage of the GCPS based on central inverter with dual-stage single-string power processing stages. The converter topology is the Step-Up DC-DC Converter with a Three-Phase High-Frequency Transformer (SDCTHT) [15] and the PV modules arrangement is 3x15 (vide Sect. III).

A. Range of Operation of PV Array

Energy generated by the photovoltaic modules is directly dependent on temperature and irradiation. Due this, a wide range of irradianations and temperatures have been considered to estimate the input voltage range [12].

The 3x15 arrangements of PV modules have been considered for this estimative. For such analysis we assume a variation of irradiation from 100 W/m² to 1000 W/m², and a variation of temperature from 0° C to 70° C. Table V shows the power and voltage at maximum power point (V_{MPP}) and the open circuit voltage (V_{OC}) for this arrangement. As can be seen, the input voltage range at MPPT is between 34.14 V and 58.49 V, but the converter may operate with input voltages up to 71.07 V.

B. Converter Design

Fig. 6 shows the topology of the SDCTHT converter, whose details about operation modes, operation stages, design procedure and converter modeling are given in [15].

SDCTHT converter is designed to always operate in the region R_2 [15]. The transformer ratio n must be designed to comply with the R_2 range ($0.33 \leq D \leq 0.66$) in all operational range of V_{in} and V_o . So n had been designed considering the

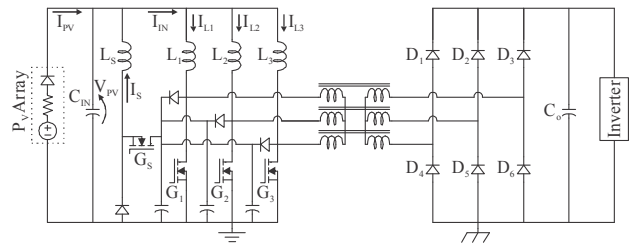


Fig. 6. Three-phase step up isolated DC-DC Converter.

maximum and minimum values of the input voltage V_{in} and the output voltage V_o , given in Table VI:

$$n = \frac{V_o(1-D)}{V_{in}} = 4 \quad (1)$$

which result in $0.35 \leq D \leq 0.62$.

Inductances are defined considering the specification for the maximum current ripple in I_{IN} ($D = 0.5$):

$$L_1 = L_2 = L_3 = \frac{V_o}{12n\Delta I_{in}f_s} = 187.5\mu H \quad (2)$$

Output capacitor is designed from the specification of the maximum ripple in DC bus [17]:

$$C_o = \frac{2.(P_o/2\omega_1)}{(V_o + \Delta V_o/2)^2 - V_o^2} = 4.28mF \cong 4.7mF \quad (3)$$

Finally, the input capacitor design considers the maximum ripple in PV array [18]:

$$C_i = \frac{\Delta I_{in}}{24f_s\Delta V_{in}} = 83.33\mu F \cong 100\mu F \quad (4)$$

V. EXPERIMENTAL RESULTS

Experimental results are presented to validate the design methodology for the SDCTHT converter described in this paper. As presented in Sect. V, the nominal power of the prototype build is 1500W due to limitation of the number of PV modules. However, experimental results were performed at 550W/48V due to limitations of the DC power source.

Fig. 7 presents the input current and the individual current of each inductor. One can observe that input current ripple is about 2A, as specified in **Error! Reference source not found.**

Fig. 8 presents the current I_{PV} , voltage and power. One can observe a low frequency ripple. This ripple is due to the DC voltage source that was used for testing. However, their average values agree with simulation results.

Fig. 9 presents the input current, PV current and the current of the snubber, this explain the difference between the input current and the PV current level. Fig. 10 presents the current and the power consumed by the first module of

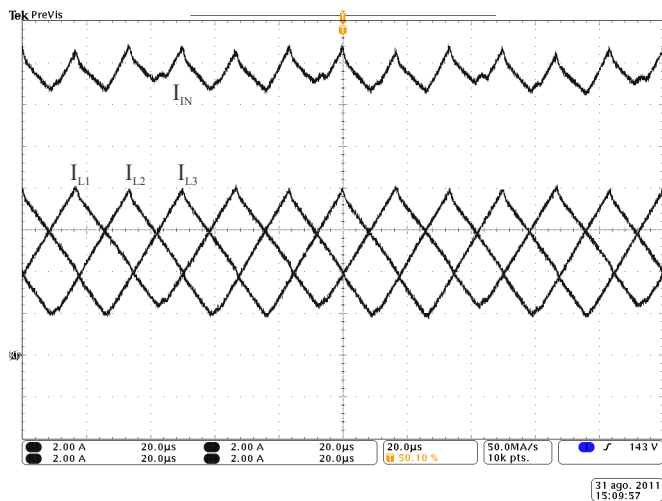


Fig. 7. Experimental results: input current and inductor's currents.

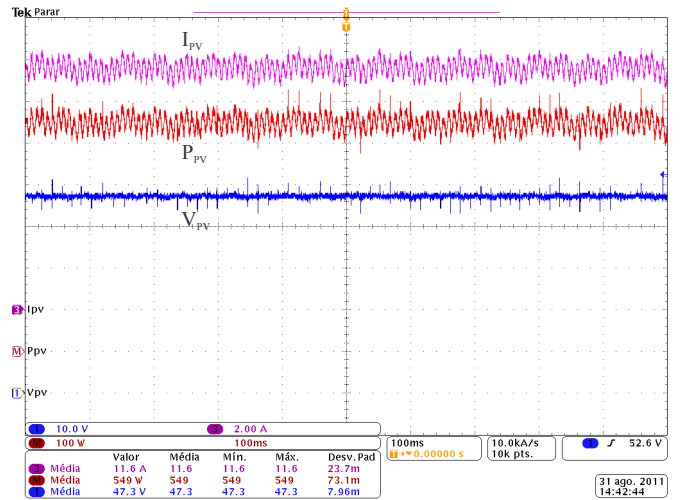


Fig. 8. Experimental results: PV current, input voltage and input power.

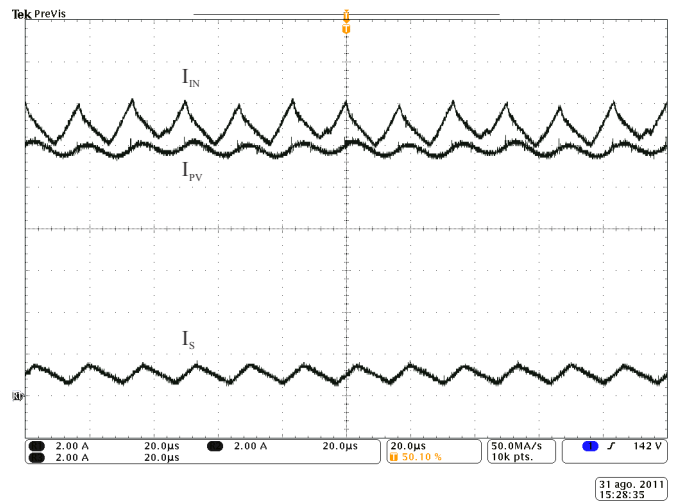


Fig. 9. Experimental results: Input current, PV current and snubber current.

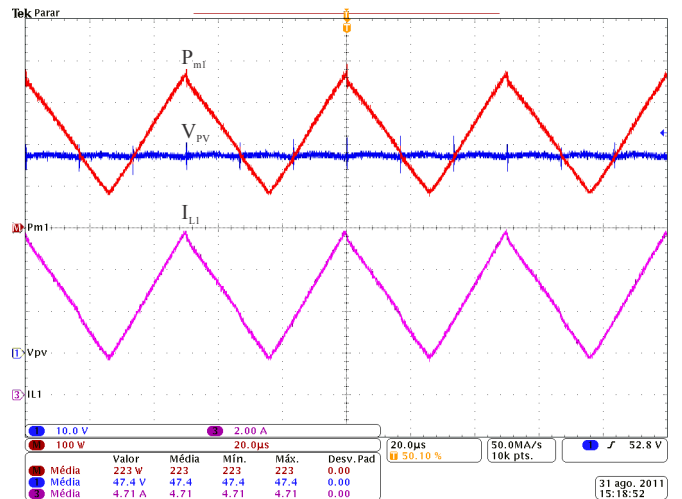


Fig. 10. Experimental results: Output voltage, output current and output power.

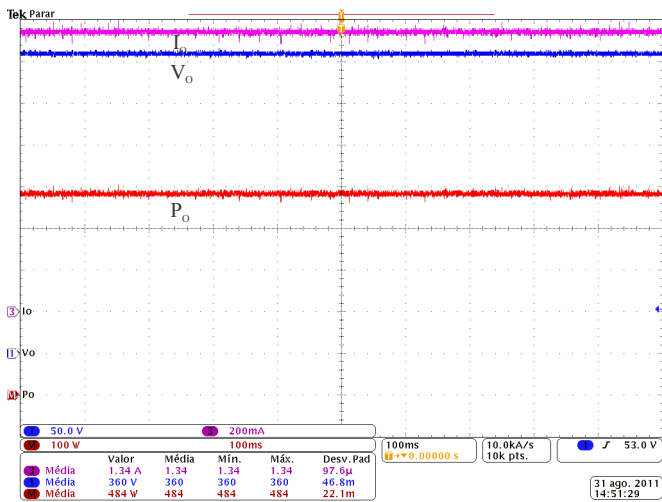


Fig. 11. Experimental results: Output voltage, output current and output power.

inductor and switch corresponding to L_1 and G_1 , one can note that the power is about 220W, this is because the increase of the current due to the snubber circuit as shown in Fig. 9. The other modules have similar waveforms. Fig. 11 presents the output current, voltage and power of the SDCTHT converter.

Preliminary results show that the efficiency of this converter is around 88% at 550W.

VI. CONCLUSIONS

This paper proposes a grid-connected photovoltaic system for residential application based in central inverter with dual-stage single-string topology. The comparative analysis of the input stage shows that most cases under partial shading parallel arrangements of PV modules result in higher fill factor than using series one. It is also demonstrated that FF of parallel arrangement is not significantly lower than in multi-string ones for arrangements with few PV modules in series.

From this analysis is designed a Step-Up DC-DC Converter with a Three-Phase High-Frequency Transformer. This topology offers important features for PV applications as high voltage gain, galvanic insulation and reduced input current ripple. Moreover, this converter have other advantageous features, such as reduced number of components, only three active switches with a single voltage reference, and high transformer utilization factor.

Simulation and experimental results are presented to validate the proposed system.

ACKNOWLEDGMENT

The authors would like to thanks to FAPESC, FAPERGS and CAPES/PROCAD for financial support.

REFERENCES

- [1] H. Yan, Z. Zhou and H. Lu, "Photovoltaic industry and market investigation", *SUPERGEN'09*, pp. 1-4, April 2009.
- [2] X. Wang, J. Gao, W. Hu, Z. Shi, B. Tang, "Research of effect on distribution network with penetration of photovoltaic system", *Universities Power Engineering Conference (UPEC)*, pp. 1-4, August/September 2010.
- [3] D. B. Cândido, J. R. R. Zientarski, R. C. Beltrame, J. R. Pinheiro, L. Michels, H. L. Hey, "Implementation of a stand-alone photovoltaic

- system based on decentralized dc-dc converters", *SOBRAEP Transactions*, vol. 15, no. 3, pp. 220-228, August. 2010.
- [4] J. Higbee, J. Brehm, P. K. Sen, R. Ammerman, "Residential electric power systems: implications for distributed generation", *Annual North American Power Symposium*, pp. 475- 480, October 2005.
- [5] I. Weiss, P. Sprau, P. Helm, "The German PV solar power financing schemes reflected on the German PV market", *3rd World Conference on Photovoltaic Energy Conversion*, vol. 3, pp. 2592- 2595 May 2003.
- [6] Trends in Photovoltaic Applications: Survey report of Selected IEA Countries between 1992 and 2009.
- [7] J. M. A. Myrzik, M. Calais, "String and module integrated inverters for single-phase grid connected photovoltaic systems - a review", *IEEE Power Tech Conference Proceedings*, vol. 2, June 2003.
- [8] J. Imhoff, J. R. Pinheiro, J. L. Russi, D. Brum, R. Gules, H. L. Hey, "DC-DC converters in a multi-string configuration for stand-alone photovoltaic systems", *IEEE PESC 2008*, pp. 2806-2812, June 2008.
- [9] Q. Xu, L. L. Lai, N. Tse, K. Ichiyangi, "Hybrid behaviors analysis of photovoltaic array performance", *International Conference on Machine Learning and Cybernetics*, vol.6, pp. 3448-3456, July 2009.
- [10] S. B. Kjaer, J. K. Pedersen, F. Blaabjerg, "A Review of Single-Phase Grid-Connected Inverters for Photovoltaic Modules", *IEEE Trans. on Industry Applications*, vol. 41, no. 5, pp. 1292-1306, September/October 2005.
- [11] L. Gao, R. A. Dougal, L. Shengyi, A. P. Iotova, "Parallel-Connected Solar PV System to Address Partial and Rapidly Fluctuating Shadow Conditions", *IEEE Transactions on Industrial Electronics*, vol. 56, no. 5, pp. 1548-1556, May 2009.
- [12] X. Weidong, N. Ozog, W. G. Dunford, "Topology Study of Photovoltaic Interface for Maximum Power Point Tracking", *IEEE Transactions on Industrial Electronics*, vol. 54, no. 3, pp. 1696-1704, June 2007.
- [13] D. Barater, G. Buticchi, A. S. Crinto, G. Franceschini, E. Lorenzani, "A new proposal for ground leakage current reduction in transformerless grid-connected converters for photovoltaic plants", *IEEE IECON '09*, pp. 4531-4536, November 2009.
- [14] Photovoltaic Module KC 130TM da Kyocera. Available at: www.kyocerasolar.com/pdf/specsheets/KC130TM.pdf
- [15] S. V. G. Oliveira, I. Barbi, "A Three-phase Step-Up DC-DC Converter with a Three-Phase High-Frequency Transformer for DC Renewable Power Sources Applications", *IEEE Transactions on Industrial Electronics*, (to appear, available in ieeexplore.ieee.org).
- [16] IEEE Guide for Terrestrial Photovoltaic Power System Safety, *IEEE Std 1374-1998*, 1998.
- [17] C. Rodriguez, G. A. J. Amaratunga, "Energy control for long lifetime photovoltaic ac module inverter", *IEEE PESC '06*, pp. 1-6, June 2006.
- [18] J. M. Kwon, B. H. Kwon, K. H. Nam, "High-efficiency module-integrated photovoltaic power conditioning system", *IET Power Electronics*, vol. 2, no. 4, pp. 410-420, July 2009.